Atmos. Chem. Phys. Discuss., 13, 3957–3992, 2013
www.atmos-chem-phys-discuss.net/13/3957/2013/
doi:10.5194/acpd-13-3957-2013

Atmospheric Chemistry and Physics Discussions

Stratospheric and tropospheric SSU/MSU temperature trends and compared to reanalyses and IPCC CMIP5 simulations in 1979–2005

A. M. Powell Jr.[1], **J. Xu**[2], **C.-Z. Zou**[3], **and L. Zhao**[4]

[1]NOAA/NESDIS/STAR, College Park, MD, USA
[2]Environmental Science and Technological Center, College of Science, George Mason University, Fairfax, VA, USA
[3]NOAA/NESDIS/STAR, College Park, MD, USA
[4]Nanjing University of Information Science and Technology, Nanjing, China

Received: 20 November 2012 – Accepted: 7 January 2013 – Published: 13 February 2013

Correspondence to: J. Xu (jianjun.xu@noaa.gov) and A. M. Powell Jr. (al.powell@noaa.gov)

Published by Copernicus Publications on behalf of the European Geosciences Union.

Abstract

Using the satellite temperature measurements from the Stratospheric Sounding Units (SSU) and Microwave Sounding Units (MSU including the advanced microwave sounding unit, AMSU) since 1979, the trends and uncertainties in the fifth Coupled Model Intercomparison Project (CMIP5) model simulations from the middle troposphere to the upper stratosphere (5–50 km) have been explored. The temperature trend discrepancies between the new generation reanalyses are investigated. Both the temporal character of the global mean temperature and the regional spatial pattern of the temperature trends are discussed. The results show that the CMIP5 model simulations reproduced common stratospheric cooling and tropospheric warming features although a significant discrepancy among the selected models was observed.

For the temporal variation of the global mean temperature, the CMIP5 simulations reproduce the volcanic signal and were highly consistent with the SSU measurements in the upper stratosphere. In contrast, the CFSR and MERRA reanalyses (excluding ERA-I) exhibit a different result from the CMIP5 simulations. For the spatial variation of the temperature trends, the CMIP5 simulations displayed a different latitudinal-longitudinal pattern from SSU/MSU measurements in all six layers from the middle troposphere to the upper stratosphere. The CFSR reanalysis shows a good spatial correlation with satellite observations in the troposphere but poor spatial correlation in the stratosphere. The ERA-I and MERRA reanalyses have good spatial correlation in the upper stratosphere and an even better spatial correlation in the troposphere.

Generally, the CMIP5 simulations significantly underestimated the stratospheric cooling in the tropics and substantially overestimated the cooling over the Antarctic in the MSU observations. The largest trend spread among the seven CMIP5 simulations is seen in both the south- and north-polar regions in the stratosphere and troposphere. The tropospheric spread values are generally smaller than the stratospheric spread values.

ACPD
13, 3957–3992, 2013

1 Introduction

The temperature variability and trends in the middle-upper atmosphere are defined by the layers from the middle troposphere to the upper stratosphere. These layers receive a great deal of attention in the climate change community, because these trends, anomalies, and variations provide evidence of natural and anthropogenic climate change mechanisms. In addition, the variation in the upper atmosphere through top-down and bottom-up forcing approaches indicate the pattern and magnitude of the impacts on the lower tropospheric and surface regional climate (Meehl et al., 2009; Seidel et al., 2011; Sigmond and Scinocca, 2010; Scaife et al., 2011; Powell and Xu, 2011; Karpechko and Manzini, 2012; Xu and Powell, 2012a). The largest climate change program, the Intergovernmental Panel on Climate Change (IPCC), made an incredible effort to understand the variability in the upper atmosphere based on climate model simulations. Compared to the third phase of the Coupled Model Intercomparison Project (CMIP3), many models of the fifth phase of the Coupled Model Intercomparison Project (CMIP5) increased the model top above 1 hPa to improve the representation of atmospheric change in the upper layers (Taylor et al., 2012; Charlton-Perez et al., 2012) in the coupled climate models. However, the reliability of these new climate model products in the upper atmosphere is still not completely clear as demonstrated by the differences between the model outputs (Räisänen, 2007; Thompson et al., 2012). Also, many of the climate models do not include all the physical and chemical processes necessary for simulating the stratospheric climate (Taylor et al., 2012). As a consequence, testing and evaluating the climate model results with integrated observational data sets is necessary to understand the capabilities and limitations in representing climate change, short term variability, and understanding how well each model captures the fundamental physics.

Generally, the set of radiosonde observations is used as the in-situ atmospheric benchmark to measure climate model performance (Santers et al., 1999; Christy et al., 2006; Sakamoto and Christy, 2009; Xu and Powell, 2010). However, the radiosonde

ACPD
13, 3957–3992, 2013

datasets exhibit uncertainties and limitations; they typically cannot penetrate to layer pressures at 20 hPa or higher and do not generally cover the ocean and the polar area coverage is limited. In addition, there have been many changes in instrumentation and observational practices, so that the raw radiosonde data record contains substantial non-climate heterogeneities (Parker and Cox, 1997; Lanzante et al., 2003). Fortunately, satellite observations overcome the shortcoming in the radiosonde observations in certain aspects. Satellite instruments not only provide data to the upper stratosphere (50 km), but also cover the ocean and polar areas consistently. The satellite observations from the Stratospheric Sounding Units (SSUs) and Microwave Sounding Units (MSUs), including the Advanced Microwave Sounding Unit (AMSU) which started taking observations in 1998, flew on US National Oceanic and Atmospheric Administration (NOAA) polar-orbiting environmental satellites between 1979 and 2005. MSU and AMSU instruments provide key observations to assess climate change (Christy et al., 2000; Mears et al., 2003; Zou et al., 2009) and the performance of climate model simulations (Santer et al., 1999; Xu and Powell, 2012b,c). Unfortunately, the number of satellite instruments, along with changes in instrument design impact observational practices and the application of the data. For example, the MSU/AMSU data come from more than 12 different satellites and the data quality is significantly affected by intersatellite biases and uncertainties in each instrument's calibration coefficients, changes in instrument body temperature, drift in sampling the diurnal cycle, roll biases and the orbital altitude decay (Christy et al., 2000; Zou et al., 2009). While methods to correct for these deficiencies have been implemented, their implementation in observational data sets and models is imperfect.

With a growing interest in climate research in recent years, the reanalysis data sets have been popularly used in climate comparison analyses (Kanamitsu et al., 2002; Trenberth, 2001; Xu and Powell, 2010). The community has noted that reanalyses are different from climate models. The fact that the reanalyses are based on the complete physical processes and constrained by the most complete integrated observation sets over the last three decades, and the climate models are driven by observed climate

ACPD
13, 3957–3992, 2013

forcing to a large extent, there is reason to expect the climate models should reflect similar features, geographical placement, and trends as portrayed in the reanalyses through the same period.

The reanalyses are continually updated gridded data sets representing the state of the Earth's atmosphere, incorporating an integrated set of observations while using a numerical weather prediction (NWP) model to ensure physical consistency. This integrated analysis interprets conflicting observations and fills gaps in observational coverage while maintaining an appropriate atmospheric structure. To increase the reanalysis capability, the new generation of reanalyses, such as CFSR, ERA-I, MERRA provide detailed information in the upper stratosphere. Even so, the reanalysis products exhibit a number of uncertainties and deficiencies when inter-compared.

For these reasons, an investigation of the temperature trends in the middle-upper atmosphere from the middle troposphere to the upper stratosphere using satellite observations, reanalyses and the CMIP5 simulations was undertaken using the same way for analyses. The goal is to understand the uncertainties and deficiencies for the estimating temperature trends in the CMIP5 simulations. Section 2 describes the data sets and methodologies. The temporal analysis of the global mean temperature and the spatial variation pattern of the global temperature trend are presented in Sects. 3 and 4, respectively. Section 5 provides a final summary and discussion.

2 Data and methodology

To assess the middle-upper atmospheric temperature trends in the CMIP5 climate model simulations, the satellite observations including the SSU and MSU measurements and the new generation reanalysis products were used for comparison. All data sets spanned the period from 1979 through 2005.

ACPD
13, 3957–3992, 2013

2.1 SSU data sets

The Stratospheric Sounding Unit (SSU) data set was developed by the Center for Satellite Applications and Research (STAR) in the National Oceanic and Atmospheric Administration (NOAA) (Wang et al., 2012). The SSU is a three-channel infrared (IR) radiometer designed to measure temperatures in the middle to upper stratosphere (Fig. 1): SSU1 (peak at ∼ 32 km), SSU2 (∼ 37 km), and SSU3 (∼ 45 km). The SSU is part of the Television Infrared Observation *Satellite* (TIROS) Operational Vertical Sounder (TOVS) instrument suite aboard NOAA Polar Orbiting Environmental Satellites (POES). The three SSU weighting functions can be seen in Fig. 1 along with the MSU weighting functions.

2.2 MSU data sets

The MSU temperature dataset was created in STAR by Zou et al. (2006, 2009). To reduce the biases in the intersatellite MSU instruments, Zou et al. (2006, 2009) developed an intercalibration method based on the simultaneous nadir overpass (SNO) matchups. Due to orbital geometry, the SNO matchups are confined to the polar region. But the integrated SNO techniques remove global intersatellite biases providing a more consistent and integrated analysis (Zou and Wang, 2011). Three of the MSU channels extend from the middle troposphere to the lower stratosphere (Fig. 1): MSU2 (∼ 6 km), MSU3 (∼ 11 km), and MSU4 (∼ 18 km).

2.3 Reanalysis data sets

Table 1 lists the reanalysis data sets used in this study. It clearly shows the different data assimilation systems, different model resolutions, model top levels in each individual reanalysis product. The NCEP Climate Forecast System Reanalysis (CFSR) is the latest version completed from 1979 through 2009 using the Gridpoint Statistical Interpolation (GSI) data assimilation system and the Community Radiative Transfer Model (CRTM)

ACPD
13, 3957–3992, 2013

developed by the Joint Center for Satellite Data Assimilation (JCSDA) for radiance data based on a global, high resolution, coupled atmosphere-ocean-land surface-sea ice system (Saha et al., 2010). ERA-I (Simons et al., 2007) is a new ECMWF reanalysis product from 1979 to the present. It was derived using a 4D-Variational (4D-Var) data assimilation system based on a newer version of the forecasting system, the Integrated Forecasting System (IFS). MERRA (Rienecker et al., 2011) covers the period from 1979 to the present and was created by Goddard Space Flight Center (GSFC). It is based on a new version of the Goddard Earth Observing System Data Assimilation System (GEOS-5), that includes the Earth System Modeling Framework (ESMF)-based GEOS-5 Atmospheric General Circulation Model (AGCM) and the new NCEP unified grid-point statistical interpolation (GSI) analysis scheme. The native resolution of MERRA is 2/3 degree longitude by 1/2 degree latitude with 72 levels extending to 0.01 hPa.

2.4 CMIP5 simulations

The analysis uses the CMIP5 climate model simulations from the IPCC Model archive at the Program for Climate Model Diagnosis and Intercomparison (PCMDI) (Taylor et al., 2012). The requirement for detailed information of the upper stratosphere for this analysis was met by seven models (Table 2) from the 22 available groups in the "historical" run. These seven CMIP5 simulations are used in this study. The "historical" run (1860–2005) is forced by observed atmospheric composition changes (reflecting both anthropogenic and natural sources) including time evolving land cover. The CMIP5 models chosen for this analysis were those where the model tops were 10 hPa or higher and provided sufficient height in the stratosphere to test the value of the data from the SSU.

ACPD
13, 3957–3992, 2013

2.5 Methodology

For each individual monthly data set listed above, the monthly zonal-mean data is interpolated to the same resolution in 10-degree latitude intervals. To facilitate inter-comparison of the same type of data, the pressure-level CMIP5 model simulation and reanalysis data are converted to layer temperatures based on the vertical weighting function of the SSU/MSU measurements (Fig. 1).

Two types of correlations are provided for the comparison of the CMIP5 simulations with the SSU/MSU/AMSU observations and reanalysis products. One is the temporal-correlation based on the global mean temperature, another is the spatial-correlation based on the global pattern of temperature trends.

The fitting of linear least squares is used to estimate the temperature trend. The model trend uncertainty is measured by the ensemble spread, which is defined by the standard deviation among seven CMIP5 climate model simulations. The *t*-test analysis is employed to calculate the statistical significance at 95 % confidence level of the temperature trends.

3 Temporal characteristics on the time variation of global mean temperature

This analysis uses the STAR produced SSU/MSU observations as the reference for comparing the reanalyses and the CMIP5 climate models. References to the SSU/MSU data set or observations throughout the remainder of this paper refers to this data set.

3.1 Global mean temperature

Figure 2 shows the time series of global mean temperature anomalies based on the satellite SSU/MSU observations, the data changes with each different vertical layer over the period from 1979 through 2005. The three SSU channels and MSU channel 4 (MSU4) in the stratosphere (Fig. 2a–d) indicate a similar interannual variability with a cooling temperature trend rate of approximately $-1.08\,^{\circ}\mathrm{C}\,\mathrm{decade}^{-1}$ in the upper

ACPD
13, 3957–3992, 2013

stratosphere (SSU3) and −0.28 °C decade^{-1} in the lower stratosphere (MSU4). It is clear that all three SSU and MSU4 channels displayed strong anomalies during the 1982–1983 and 1991–1992 periods, which correspond to the volcanic eruptions of El Chichon (1982) and Mt. Pinatubo (1991).

In comparison, the troposphere (Fig. 2e, f) shows a weak warming at a rate of +0.10 °C decade^{-1} in the upper troposphere (MSU3) and 0.16 °C decade^{-1} in the middle troposphere (MSU2). In these upper troposphere channels, it is harder to identify the connection with the volcanic eruptions due to the decreased sensitivity of these channels to volcanic effects in the troposphere. However, it is worth noting that the tropospheric temperature (MSU2 and MSU3) shows a close relationship with El Niño and La Niña events (Fig. 2e, f).

Compared to the satellite SSU observations, the CFSR (red line in Fig. 3a–c) shows significantly different features in the upper stratosphere. The upper stratospheric temperature anomaly in the CFSR displayed large amplitude changes compared to the SSU observations while a relatively weak abnormal variation was observed in the MERRA (dark blue line). It is obvious that the abnormal amplitude in the reanalysis is not coming from the volcanic eruptions. However, all three reanalyses show high consistency with MSU observations from the middle troposphere (MSU2) to the lower stratosphere (MSU4) (Fig. 3d–f).

For the CMIP5 simulations, all seven of the selected climate models reproduced the temperature variability in the stratosphere (Fig. 3a–d) except the MRI-CGCM3 overestimated the temperature response to the Mt. Pinatubo volcano in 1991–1992. In contrast, three models (MIROC4h, MPI-ESM-LR, and MRI-CGCM) show a significant discrepancy from the MSU observations in the troposphere (Fig. 3e–f). Most of these models did not reflect the El Niño/El Niña signals observed in the MSU observations (Fig. 2e, f).

ACPD
13, 3957–3992, 2013

3.2 Temporal correlation

The comparison of the global mean temperature from the SSU/MSU observations with the CMIP5 models and the reanalyses is accomplished through temporal correlation to measure the performance of these climate model simulations. In Table 3, when the correlation coefficient exceeds the threshold value of 0.5, it indicates that 25 % or more of the variance in the datasets is explained by the correlation, and satisfies the statistical significant test at the 99 % confidence level.

In the stratosphere (Table 3), the temporal correlations between SSU/MSU and CMIP5 climate models have a higher correlation coefficient ranging from 0.76 to 0.98, which reflects the strong consistency of the global mean stratospheric temperature in the CMIP5 climate model simulations. It is clear that the selected seven CMIP5 climate models effectively reproduced the time variation of the global mean stratospheric temperature in the upper stratosphere. However, the correlations with the reanalyses are apparently lower than the climate model simulations. The correlation coefficient for the SSU3 layer in the CFSR data is down to 0.38; it reflected the large discrepancy in the global mean temperature time series (Fig. 3a). Note the correlation values in the ERA-I are substantially higher than the other two reanalyses (MERRA and CFSR). This suggests our European partners have more consistent data assimilation schemes across different satellites in their models whether NWP or climate based.

In the troposphere, contrastingly, the MSU observation correlations with the CMIP5 model simulations are sharply reduced. There are only two temporal-correlations larger than 0.5 which exceed the 99 % significance test; this demonstrates a poor similarity to the MSU in the CMIP5 simulations, which indicates that the CMIP5 simulations in the troposphere are worse than those in the stratosphere. However, the MSU temporal-correlations with the reanalyses are remarkably increased, which shows the reanalyses have much better performance in the troposphere than their counterpart climate models in the stratosphere.

ACPD
13, 3957–3992, 2013

3.3 Trends and spread change with vertical level

The vertical profile of the global mean temperature trends shows (Fig. 4) a clear similarity between the CMIP5 model simulations (Fig. 4a) and the reanalyses (Fig. 4b) where the cooling rate of the temperature trends in the upper stratosphere are less than the SSU observations. The crossover points identify a transition from tropospheric warming to stratospheric cooling. In both cases, the CMIP5 simulations and the reanalyses are lower than the corresponding crossover point from the MSU observations. In other words, the warming rates in the troposphere are less than those in the MSU observations (STAR SSU/MSU data set). On the other hand, the ensemble spread among the CMIP5 model simulations (lower left corner in Fig. 4a) are generally between −0.4 and $-0.8\,^{\circ}\mathrm{C\,decade^{-1}}$ from middle troposphere to upper stratosphere, with the maximum spread appearing at the peak point of the SSU3 level (∼ 45 km). The large spread is mainly due to the underestimation of the cooling trend in MIROC4h. In the reanalyses, the ensemble spread (lower left corner in Fig. 4b) substantially decreases with height with the maximum value reaching an approximate value $-1.0\,^{\circ}\mathrm{C\,decade^{-1}}$ for SSU1 and SSU2. It is obvious that the large spread in the upper stratosphere is coming from the discrepancy between CFSR and MERRA. The discrepancies are created because the CFSR has a spurious trend generated from the integration methods used in the model.

Compared to the new generation reanalyses, the above results clearly show that the global mean temperature variability in CMIP5 simulations have their highest consistency with the SSU/MSU observations in the stratosphere. In contrast, the reanalysis shows a relatively strong correlation in the troposphere. The reanalysis is apparently better than the CMIP5 simulation for the temperature variability in the troposphere and displays an increasing temperature trend. In addition, the reanalyses show a relatively weak correlation with SSU/MSU observations in the stratosphere, which reflects to some degree, the limitation of data assimilation in the upper stratosphere. Note that the transition (crossover) point where the tropospheric warming changes into stratospheric

ACPD
13, 3957–3992, 2013

cooling is a little above MSU3. The heights of the crossover point in both CMIP5 simulations and reanalyses are lower than in the STAR MSU observation data set. Obviously, the difference will impact the estimation of temperature trends. The result implies that the CMIP5 climate model simulations and the reanalyses overestimated (underestimated) the tropospheric warming (stratospheric cooling) compared to the STAR MSU observations.

4 Spatial pattern for the regional variation of temperature trends

4.1 Longitude-latitude distribution

Figure 5 displays the latitudinal-longitudinal variation of the global temperature trends for 1979–2005 for the layers from the middle troposphere (~ 6 km height) to the upper stratosphere (~ 48 km height).

For the SSU/MSU observations (left panel in Fig. 5), the latitudinal-longitudinal distributions of temperature trend are changing with vertical level. Strong cooling is clearly observed in the upper stratosphere (SSU1~SSU3) in the tropical and subtropical areas, while strong warming appeared in the middle troposphere in both the tropics and most of the Northern Hemisphere. The strongest warming was on the order of 0.5 °C decade^{-1} occurring at the middle troposphere (MSU2) in northern high latitudes. The largest cooling trend in the upper stratosphere (SSU3) exceeds −1.4 °C decade^{-1} in the tropical and northwestern Arctic areas. It is worth noting that the magnitude of the temperature trend is apparently sensitive to the position in its three dimensional atmosphere.

For the reanalysis (middle panel in Fig. 5), the temperature trends in the CFSR reanalysis (MERRA and ERA-I are not shown; see Appendix for their results) show a similar pattern to the SSU/MSU observations from the troposphere to stratosphere at all six levels. The cooling in the upper stratosphere in the tropical zone is much weaker than the SSU observations. Relatively strong warming was contrained to the tropical zone in

ACPD
13, 3957–3992, 2013

the troposphere, while the cooling in both Arctic and Antarctic zones substantially expanded to the middle latitudes, especially in the Arctic zone in the upper troposphere (MSU3). Note the cooling pattern in the upper stratosphere is similar to the SSU observations although the time variation of the global mean temperature is different from the SSU3 observations (Fig. 3a).

For the CMIP5 simulations (right panel in Fig. 5), a randomly selected model MPI-ESM-LR (the other six model results are shown in the appendix) simulation shows basically cooling in the stratosphere and warming in the troposphere. However, the latitudinal-longitudinal pattern of the trends is remarkably different from the SSU/MSU observations.

Generally, the stratospheric cooling is underestimated in the tropics in both CMIP5 simulations and reanalyses compared to the SSU observations. The reanalyses show a large rate of cooling in the southern polar region in the troposphere.

4.2 Spatial correlation

To quantify the similarities and differences between model simulations and observations, the spatial correlations and the temperature trend change with latitude was calculated. The spatial correlations between the reanalyses and the SSU/MSU observations indicate (Fig. 6) that the reanalyses in both the stratosphere and troposphere are in very good agreement with the satellite observations except for the ERA-I and MERRA in the upper stratosphere (SSU3). The CMIP5 simulations have a smaller correlation than the reanalyses especially in the troposphere, while the model MICRO-ESM-CHEM for the three SSU channels shows a negative correlation with the SSU observations. The MICRO4h model simulations in the upper stratosphere look better than the other six models.

Three points in the spatial correlation are worth noting: (1) the CFSR has a very weak temporal correlation for the global mean temperature, but shows a strong spatial correlation in the upper stratosphere. In contrast, ERA-I shows the opposite effect. (2) All seven CMIP5 models show good temporal correlation in the stratosphere, but show

ACPD
13, 3957–3992, 2013

poor spatial correlation except for the MIROC4h, where both the temporal and spatial correlations are very poor in the troposphere. (3) The MICRO-ESM-CHEM model which includes a chemistry model shows a poorer correlation in the upper stratosphere than the MICRO4h model which excludes the chemistry modeling.

4.3 Trends and spread change with latitudes

To best understand the spatial pattern of the CMIP5 model simulations, the latitude profiles of the temperature trend have been graphed to facilitate comparing the differences between the datasets. The results indicate (Fig. 7) that the linear trends are highly sensitive to the latitude of interest. All exhibit predominant cooling in the stratosphere and warming in troposphere except for the southern high latitudes. Also, there is an extremely strong cooling trend in the three SSU channel observations over the tropics and subtropics.

For the upper stratosphere (Fig. 7a–c), a distinguishing difference in the SSU observations from the CMIP5 simulations and reanalyses is found over the tropics, where the cooling rates get up to 1.6 K decade^{-1} in the SSU3 layer (Fig. 7a). This is approximately −0.5 K decade^{-1} lower than the value in the CMIP5 models and the reanalyses In addition, the cooling trend shows a sharp gradient from high to lowlatitude in SSU observations.

For the layer from the middle troposphere to the lower stratosphere (Fig. 7d–f), the MSU data shows a consistent trend with the CMIP5 models and the reanalyses. An important fact worth noting is that a cooling was found in the troposphere over Antarctica, with the maximum cooling trend being approximately −1.0 K decade^{-1} in the upper troposphere. At the same time, warming trends have been observed over the tropics and the whole Northern Hemisphere. This layer also displayed a substantial temperature difference between the Antarctic and the rest of the areas.

Figure 8 shows the temperature spread change with latitude for the seven CMIP5 simulations. The spread in the seven CMIP5 simulations change with latitude from ∼ 0.05 K decade^{-1} in tropical and subtropical areas to ∼ 0.25 K decade^{-1} in both the

ACPD
13, 3957–3992, 2013

southern and northern polar region. The spread in stratosphere (three SSU and MSU4) gets up to 0.25–0.3 K decade^{-1} over the Antarctic, with the value being much higher than in the two MSU channels in the troposphere (0.15 K decade^{-1}). Over the Arctic, the layer spread for MSU2 is much lower than the other five upper level observation sets. In contrast, there are some remarkable discrepancies in the tropical regions in the MSU4 layer. It is worth noting that the spread of the CMIP5 simulations in the middle troposphere (MSU2) is a small value at all latitudes The smaller spread in the MSU2 reflects the high consistency in CMIP5 simulations.

It is obvious that the cooling trends of the stratospheric temperature markedly changes with latitude, and the largest trend is found in the tropics-subtropics but the largest spread is found in both south and north polar regions. In contrast, the warming trend increases with latitude from south to north in the troposphere, but the spread retains a small value except for both polar areas.

5 Summary and discussion

5.1 Summary

Based on the satellite SSU and MSU temperature observations from 1979 through 2005, the trends and uncertainties in CMIP5 model simulations and the new generation reanalyses from the middle troposphere to the upper stratosphere (5–50 km) have been examined. The results are summarized as follows:

The CMIP5 model simulations reproduced a common feature with cooling in stratosphere and warming in troposphere, but the trend exhibits a significant discrepancy among the selected seven models. The cooling rate is less than the SSU measurements changing from −0.6 to −1.0 °C decade^{-1} at the upper stratosphere, while the warming rate is generally smaller than the MSU observations changing from 0.08 to 0.24 °C decade^{-1} in the middle-upper troposphere.

ACPD
13, 3957–3992, 2013

On the temporal variation of the global mean temperature, the CMIP5 model simulations significantly reproduced the volcanic signal and was highly correlated with the SSU measurements in the upper stratosphere during the study period. However, these models do not show the impacts from El Niño/La Niña events and have poor temporal correlation with observations in the middle-upper troposphere. The reanalyses from CFSR and MERRA (excluding ERA-I) exhibit an opposite result to the CMIP5 simulations.

On the regional variation of the global temperature trends, the CMIP5 simulations displayed a different latitudinal-longitudinal pattern compared to the SSU/MSU measurements in all six layers from the middle troposphere to the upper stratosphere. Furthermore, the CMIP5 simulations show poor spatial correlations with the SSU/MSU observations. Three reanalyses showed consistent temperature patterns with the SSU/MSU observations except that they overestimated the cooling observed over both the southern and northern polar region in the upper troposphere (MSU3). The reanalyses generally show a good spatial correlation with satellite observations in all six layers with the exception of the ERA-I and MERRA reanalyses in the upper stratosphere (SSU3). Interestingly, the CFSR shows a good spatial correlation with the global temperature trends but a poor temporal correlation for the global mean temperature in the upper stratosphere. Also, the ERA-I model shows opposite temporal and spatial correlation features compared to the CFSR.

Generally, the temperature trends and spread show marked changes with latitude, the largest cooling is found in the tropics in the upper stratosphere and largest warming appears in the Arctic in the middle troposphere. The CMIP5 simulations underestimated the stratospheric cooling in the tropics compared to the SSU observations and remarkably overestimated the cooling in the Antarctic from the middle troposphere to lower stratosphere (MSU2–4). The largest trend spread among the seven CMIP5 simulations is seen in both the south- and north-polar regions in the stratosphere and troposphere. Generally, the CMIP5 simulations retain similar spread values at all latitudes in

ACPD
13, 3957–3992, 2013

both the troposphere and stratosphere. The tropospheric spread values are generally smaller than the stratospheric trend spread values.

5.2 Discussion

According to above analysis, there are two points worth noticing. (1) All seven of the selected CMIP5 model simulations showed high correlation with SSU/MSU observations in the stratosphere compared to the global mean temperature in the troposphere (Fig. 3 and Table 3), but these models failed to reproduce the latitude-longitude pattern of the temperature trends (Figs. 5 and 6). Note, all the selected CMIP5 models are coupled with land and ocean models including many kinds of physical processes focusing on the lower atmosphere, which is theoretically beneficial for describing the tropospheric atmosphere. On the other hand, most of CMIP5 models do not have some of the needed physical and chemical processes. For example, six of the seven selected CMIP5 models do not include a chemistry model in the stratosphere; only the MIROESM-CHEM includes chemistry and the chemistry model was recognized as a very important component to reproduce the true atmosphere (Meehl et al., 2009). Consequently, the climate model seems better overall in the stratosphere. Unfortunately, the above comparison shows that these CMIP5 model simulations provided a worse result in the troposphere for the global mean temperature. Given the differences noted, consider an important question: what is the key factor(s) affecting the performance of a climate model?

(2) Compared to the CMIP5 model simulation, the NCEP new generation reanalysis CFSR provided a poor estimation of global mean temperature in the upper stratosphere (Fig. 3a–c). According to the description for the CFSR reanalysis system (Saha et al., 2010), many kinds of observational data including SSU and MSU products were assimilated into the CFSR. However, the reanalysis was executed with 6 separated streams. So stream related model biases appeared to dominate in the middle and upper stratospheres where in situ observations are rare to anchor the system. In addition, the CFSR reanalysis has a good spatial correlation with the upper SSU observations for

ACPD
13, 3957–3992, 2013

the global temperature trend distribution although the temporal correlation is very poor for the global mean temperature – which is out of phase or opposes the result in the ERAI reanalysis (Table 3 and Fig. 6a). Although the reanalysis was recognized as one of the best data sets for understanding atmospheric dynamic processes by previous studies, one should consider how we can improve the reanalysis products to help us to understand climate change.

Acknowledgement. The NCEP-CFSR reanalysis data were obtained from The National Climatic Data Center (NCDC). The ERA-I reanalysis data were obtained from the European Center for Medium Range Forecasting (ECMWF). The MERRA reanalysis was obtained from the National Aeronautics and Space Administration (NASA). The SSU and MSU data sets were obtained from the Center for Satellite Applications and Research (STAR). The authors would like to thank these agencies for providing the data.

This work was supported by the National Oceanic and Atmospheric Administration (NOAA), National Environmental Satellite, Data, and Information Service (NESDIS), Center for Satellite Applications and Research (STAR). The views, opinions, and findings contained in this publication are those of the authors and should not be considered an official NOAA or US Government position, policy, or decision.

References

Charlton-Perez, A. J., Baldwin, M., Birner, T., Black, R. X., Butler, A. H., Calvo, N., Davis, N. A., Gerber, E. P., Gillett, N., Hardiman, S., Kim, J., Krueger, K., Lee. Y.-Y., Manzini, E., McDaniel, B. A., Polvani, L., Reichler, T., Shaw, T. A., Sigmond, M., Son, S.-W., Tohey, M., Wilcox, L., Yoden, S., Christiansen, B., Lott, F., Shindell, D., Yukimoto, S., and Watanabe, S.: Mean Climate and Variability of the Stratosphere in the CMIP5 models, J. Geophys. Res., in press, doi:10.1029, 2012.

Christy, J. R. and Norris, W. B.: Satellite and VIZ-radiosonde intercomparisons for diagnosis of nonclimatic influences, J. Atmos. Oceanic Technol., 23, 1181–1194, 2006.

Christy, J. R., Spencer, R. W., and Braswell, W. D.: MSU tropospheric temperatures: dataset construction and radiosonde comparisons, J. Atmos. Oceanic Technol., 17, 1153–1170, 2000.

ACPD
13, 3957–3992, 2013

Kanamitsu, M., Ebisuzaki, W., Woollen, J., Yang, S. K., Hnilo, J. J., Fiorino, M., and Potter, G. L.: NCEP–DOE AMIP-II Reanalysis (R-2), Bull. Amer. Meteor. Soc., 83, 1631–1643, 2002.
Karpechko, A. Y. and Manzini, E.: Stratospheric influence on tropospheric climate change in the Northern Hemisphere, J. Geophys. Res., 117, D05133, doi:10.1029/2011JD017036, 2012.
Lanzante, J. R., Klein, S. A., and Seidel, D. J.: Temporal homogenization of monthly radiosonde temperature data, Part I: methodology, J. Climate, 16, 224–240, 2003.
Mears, C. A., Schabel, M. C., and Wentz, F. J.: A reanalysis of the MSU channel 2 tropospheric temperature record, J. Climate, 16, 3650–3664, 2003.
Parker, D. E., Gordon, M., Cullum, D. P. N., Sexton, D. M. H., Folland, C. K., and Rayner, N.: A new global gridded radiosonde temperature database and recent temperature trends, Geophys. Res. Lett., 24, 1499–1502, 1997.
Powell, A. and Xu, J.: Possible solar forcing of interannual and decadal stratospheric planetary wave variability in the Northern Hemisphere: an observational study, J. Atmos. Solar-Terrestrial Phys., 73, 825–838, doi:10.1016/j.jastp.2011.02.001, 2011.
Räisänen, J.: How reliable are climate models?, Tellus A, 59, 2–29, 2007.
Rienecker, M. M. Michele, M., Suarez, M. J., Gelaro, R., Todling, R., Bacmeister, J., Liu, E., Bosilovich, M. G., Schubert, S. D., Takacs, L., Kim, G.-K., Bloom, S., Chen, J., Collins, D., Conatym A., da Silva, A., Gu, W., Joiner, J., Koster, R. D., Lucchesi, R., Molod, A., Owensm T., Pawson, S., Pegion, P., Redder, C. R., Reichle, R., Robertson, F. R., Ruddick, A. G., Sienkiewicz, M., and Woollen, J.: MERRA: NASA's modern-era retrospective analysis for research and applications. J. Climate, 24, 3624–3648, doi:10.1175/JCLI-D-11-00015.1, 2011.
Saha, S., Moorthi, S., Pan, H.-L., Wu, X., Wang, J., Nadiga, S., Tripp, P., Kistler, R., Woollen, J., Behringer, D., Liu, H., Stokes, D., Grumbine, R., Gayno, G., Wang, J., Hou, Y.-T., Chuang, H.-Y., Juang, H.-M. H., Sela, J., Iredell, M., Treadon, R., Kleist, D., Van Delst, P., Keyser, D., Derber, J., Ek, M., Meng, J., Wei, H., Rongqian Yang, Stephen Lord, Huug Van Den Dool, Arun Kumar, Wanqiu Wang, Long, C., Chelliah, M., Xue, Y., Huang, B., Schemm, J.-K., Ebisuzaki, W., Lin, R., Xie, P., Chen, M., Zhou, S., Higgins, W., Zou, C.-Z., Liu, Q., and Chen, Y.: Yong Han, Lidia Cucurull, Richard W. Reynolds, Glenn Rutledge, Mitch Goldberg: The NCEP climate forecast system reanalysis, Bull. Amer. Meteor. Soc., 91, 1015–1057, doi:10.1175/2010BAMS3001.1, 2010.
Sakmoto, M. and Christy, J.: The influences of TOVS radiance assimilation on temperature and moisture tendencies in JRA-25 and ERA-40, J. Atmos. Oceanic Tech., 26, 1435–1455, doi:10.1175/2009JTECHA1193.1, 2009.

ACPD
13, 3957–3992, 2013

Santer, B. D., Hnilo, J. J., Wigley, T. M. L., Boyle, J. S., Doutriaux, C., Fiorino, M., Parker, D. E., and Taylor, K. E.: Uncertainties in observationally based estimates of temperature change in the free atmosphere, J. Geophys. Res., 104, 6305–6333, 1999.

Scaife, A. A., Spanghel, T., Fereday, D. R., Cubasch, U., Langematz, U., Akiyoshi, H., Bekki, S., Braesicke, P., Butchart, N., Chipperfield, M. P., Gettleman, A., Hardiman, S. C., Michou, M., Rozanov, E., and Shepherd, T. G.: Climate-change projections and stratosphere-troposphere interaction, Clim. Dynam., 38, 2089–2097, doi:10.1007/s00382-011-1080-7, 2011.

Seidel D. J., Gillett, N. P., Lanzante, J. R., Shine, K. P., and Thorne, P. W., Stratospheric temperature trends: our evolving understanding, Wiley Interdiscip. Rev. Clim. Change, 2, 592–616, 2011.

Sigmond, M. and Scinocca, J. F.: The influence of basic state on the Northern Hemisphere circulation response to climate change, J. Climate, 23, 1434–1446, 2010.

Simons, A., Uppala, S., Dee, D., and Kobayashi, S.: ERA-Interim: new ECMWF reanalysis products from 1989 onwards, ECMWF Newslet. No. 110 – Winter 2006/07, 2007.

Taylor, K. E., Stouffer, R. J., and Meehl, G. A.: An overview of CMIP5 and the experiment design, Bull. Amer. Meteor. Soc., 93, 485–498, doi:10.1175/BAMS-D-11-00094.1, 2012.

Thompson, D. W. J., Seidel, D. J., Randel, W. J., Zou, C.- Z., Butler, A. H., Mears, C., Osso, A., Long, C., and Lin, R.: The mystery of recent stratospheric temperature trends, Nature, 491, 692–697, doi:10.1038/nature11579, 2012.

Trenberth, K. E., Stepaniak, D. P., Hurrell, J. W., and Fiorino, M.: Quality of reanalyses in the tropics, J. Climate, 14, 1499–1510, 2001.

Wang, L., Zou, C.-Z., and Qian, H.: Construction of stratospheric temperature data records from stratospheric sounding units, J. Climate, 25, 2931–2946, doi:10.1175/JCLI-D-11-00350.1, 2012.

Xu, J. and Powell, A.: Ensemble spread and its implication for the evaluation of temperature trends from multiple radiosondes and reanalyses products, Geophy. Res. Lett., 37, L17704, doi:10.1029/2010GL044300, 2010.

Xu, J. and Powell, A.: What happened to surface temperature with sunspot activity in the past 130 years?, Theor. Appl. Climatol., doi:10.1007/s00704-012-0694-y, 2012a.

Xu, J. and Powell, A.: Uncertainty estimation of the global temperature trends for multiple radiosondes, reanalyses, and CMIP3/IPCC climate model simulations, Theor. Appl. Climatol., 108, 505–518, doi:10.1007/s00704-011-0548-z, 2012b.

ACPD
13, 3957–3992, 2013

Xu, J. and Powell Jr., A. M.: Intercomparison of temperature trends in IPCC CMIP5 simulations with observations, reanalyses and CMIP3 models, Geosci. Model Dev. Discuss., 5, 3621–3645, doi:10.5194/gmdd-5-3621-2012, 2012c.

Zou, C. and Wang, W.: Inter-satellite calibration of AMSU-A observations for weather and climate applications, J. Geophys. Res., Vol. 116, D23113, doi:10.1029/2011JD016205, 2011

Zou, C., Goldberg, M., Cheng, Z.,Grody, N., Sullivan, J., Cao, C., and Tarpley, D.: Recalibration of microwave sounding unit for climate studies using simultaneous nadir overpasses, J. Geophys. Res., 111, D19114, doi:10.1029/2005JD006798, 2006.

Zou, C., Gao, M., and Goldberg, M.: Error structure and atmospheric temperature trends in observations from the microwave sounding unit, J. Climate, 22, 1661–1680, 2009.

ACPD
13, 3957–3992, 2013

Table 1. List of reanalysis data sets.

Name	Reanalysis period	Resolution	Data assimilation method	Model system	Satellite data processing
NCEP-CFS	1979–present	T382L6	3D-Var	CFS AOGCM	CRTM
ERA-I	1979–present	T255L6	4D-Var	IFS AGCM	RTTO
MERR	1979–present	2/3 × 1/2 L72	3D-Var	GEOS-5AGCM	CRTM

GFS: Global Forecast System; CFS: Climate Forecast System; IFS: Integrated Forecasting System; GEOS: Goddard Earth Observing System Data Assimilation System; GSM: Global Spectral Model; CRTM: Community Radiative Transfer Model; RTTOV: The Fast Radiative Transfer Model for TOVS.

ACPD
13, 3957–3992, 2013

Table 2. The CMIP5/IPCC data sets and selected information.

IPCC I.D.	mode	Center and location	Forcing
anESM2	atmosphere; ocean; sea ice; land	Canadian Centre for Climate Modelling and Analysis	GHG, SA, Oz, BC, OC, LU, SI, VI
HadGEM2-CC	atmosphere; ocean; lan; ocean-biogeo-chemistry	Met Office Hadley Centre	GHG, SA, Oz, BC, OC, LU, SI, VI
MIROC-ESM	atmosphere; ocean; sea ice; lan; aerosol; ocean-biogeochem-istry; land-biogeo-chemistry	Japan Agency for Marine-Earth Science and Technology	GHG, SA, Oz, BC, OC, LU, SI, VI, MD
MIROC-ESM-CHEM	atmosphere; ocean; sea ice; lan; aerosol; ocean-biogeochem-istry; land-biogeo-chemistry atmos-pheric-chemistry	Japan Agency for Marine-Earth Science and Technology	GHG, SA, Oz, BC, OC, LU, SI, VI, MD
MIROC4h	atmosphere; ocean; sea ice; land	The University of Tokyo, Japan National Institute for Environ-mental Studies and Japan Agency for Marine-Earth Sci-ence and Technology	GHG, SA, Oz, BC, OC, LU, SI, VI, MD, SS, Ds
MPI-ESM-LR	atmosphere; ocean; sea ice; land, marine	Max Planck Institute for Meteo-rology	GHG, SD, Oz, LU, SI, VI
MRI-CGCM3	atmosphere; ocean; sea ice; land; aerosols	MRI (Meteorological Research Institute, Tsukuba, Japan)	GHG, SA, Oz, BC, OC, LU, SI, VI

BC (black carbon); Ds (Dust); GHG (well-mixed greenhouse gases); LU (land-use change); MD (mineral dust); OC (organic carbon); Oz (tropospheric and stratospheric ozone); SA (anthropogenic sulfate aerosol direct and indirect effects); SD (anthropogenic sulfate aerosol, accounting only for direct effects); SI (anthropogenic sulfate aerosol, accounting only for indirect effects); SI (solar irradiance); SO (stratospheric ozone); SS (sea salt); TO (tropospheric ozone); VI (volcanic aerosol).

ACPD
13, 3957–3992, 2013

Table 3. Temporal correlation of global mean temperature between STAR SSU/MSU data set, the CMIP5 models and the reanalyses. (Stars indicate the correlation coefficient less than 0.5).

	CMIP5 Climate Model Simulations							Reanalyses		
	CanESM	HadGEM	MIROC-ESM-CHEM	MIROC-ESM	MIROC4h	MPI-ESM-LR	MRI-CGCM3	CFSR	ERA-I	MERRA
SSU3	0.96	0.97	0.97	0.97	0.83	0.97	0.93	0.38*	0.8	0.74
SSU2	0.97	0.98	0.97	0.96	0.89	0.97	0.9	0.56	0.95	0.8
SSU1	0.93	0.95	0.96	0.95	0.93	0.92	0.76	0.71	0.95	0.78
MSU4	0.9	0.89	0.87	0.88	0.9	0.9	0.8	0.93	0.97	0.98
MSU3	0.23*	0.4*	0.22*	0.15*	0.1*	0.39*	0.18*	0.77	0.89	0.88
MSU2	0.43*	0.51	0.32*	0.41*	0.36*	0.51	0.31*	0.9	0.94	0.96

ACPD
13, 3957–3992, 2013

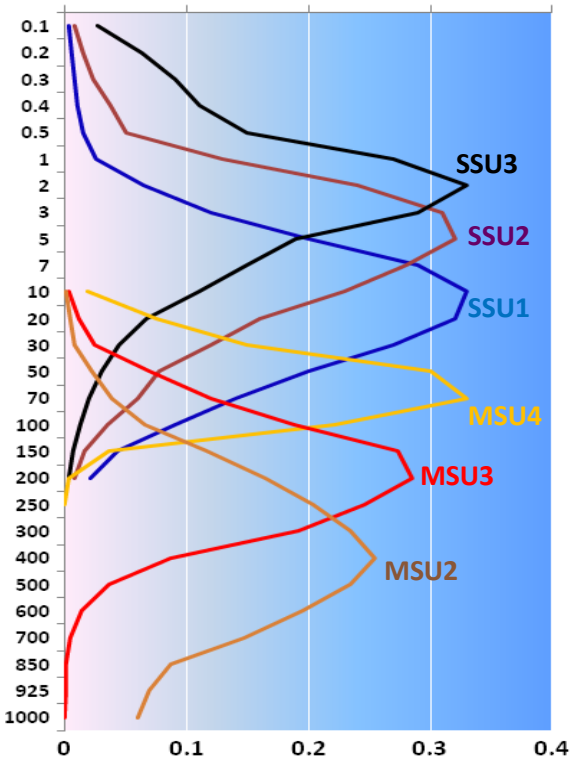

Fig. 1. Vertical weighting functions for satellite Microwave Sounding Unit (MSU) and Stratospheric Sounding Unit (SSU) temperature observations as a function of pressure.

ACPD
13, 3957–3992, 2013

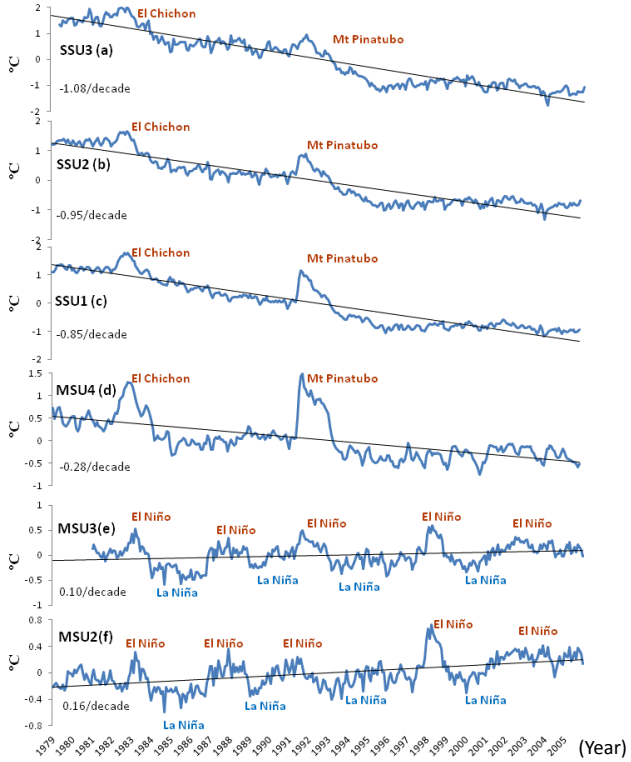

Fig. 2. Global mean temperature (˚C) in SSU/MSU observations in the period of 1979–2005.

ACPD
13, 3957–3992, 2013

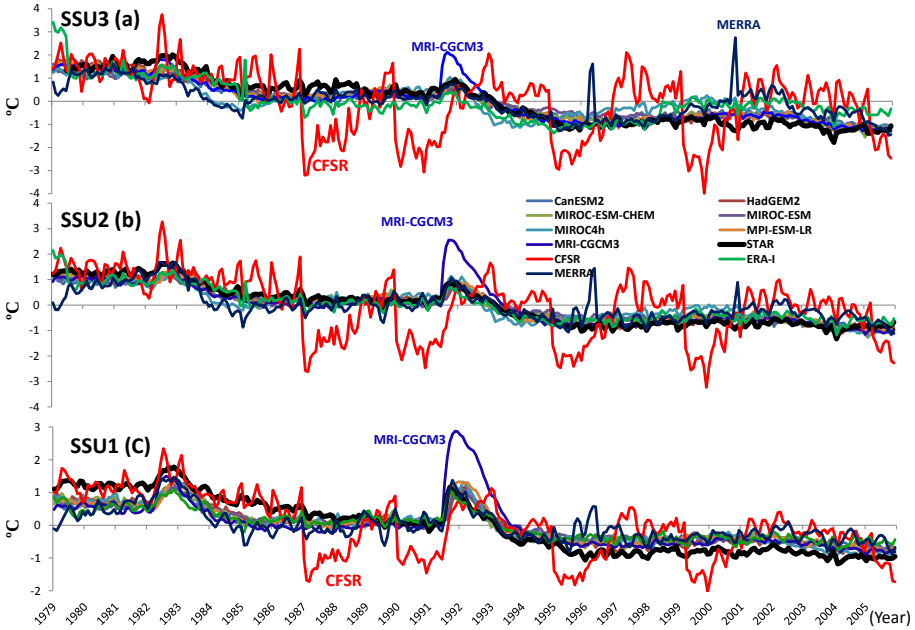

Fig. 3a. Global temperature time series (˚C) in the period of 1979–2005 at **(a)** SSU3 , **(b)** SSU2, **(c)** SSU1. Note SSU1 ~ SSU3 represent the SSU observational layers.

ACPD
13, 3957–3992, 2013

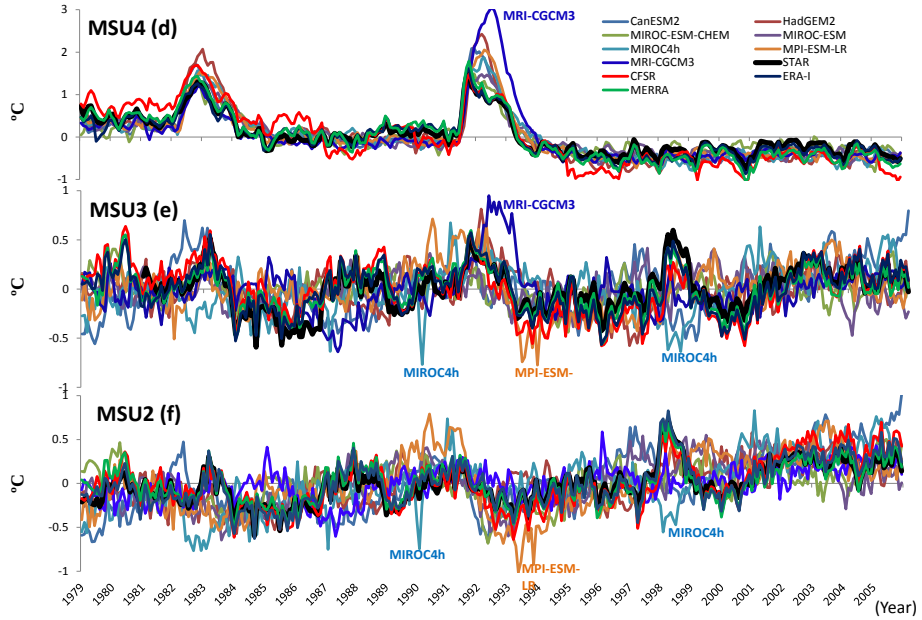

Fig. 3b. Same as the Fig. 3a except for the MSU observation **(d)** MSU4, **(e)** MSU3, **(f)** MSU2. Note MSU2 ~ MSU4 represent the MSU observational layers.

ACPD
13, 3957–3992, 2013

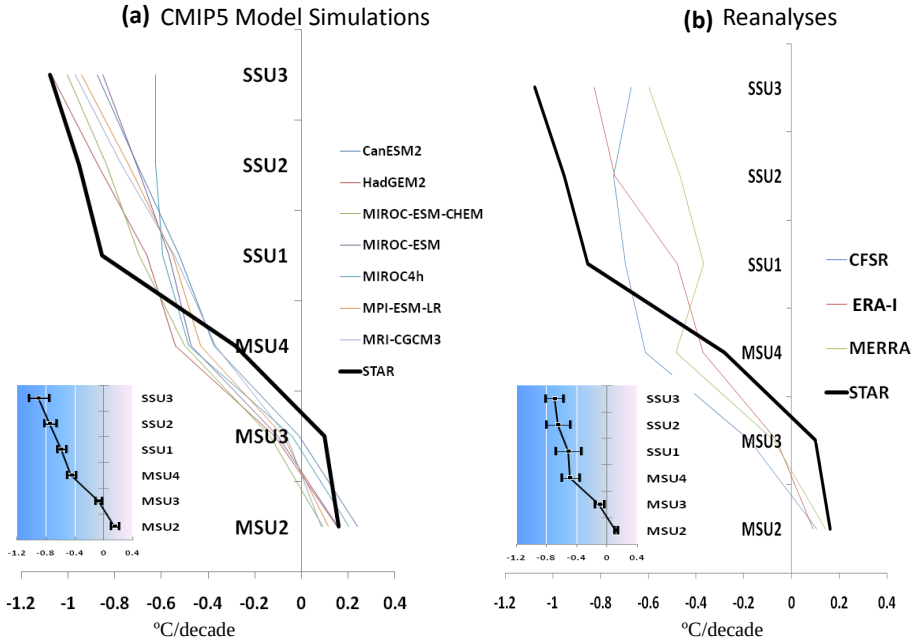

Fig. 4. Vertical profile of global mean temperature trends (°C decade^{-1}). The left lower corner represent the spread (°C decade^{-1}) among the data sets **(a)** CMIP5 model simulations, **(b)** reanalysis.

ACPD
13, 3957–3992, 2013

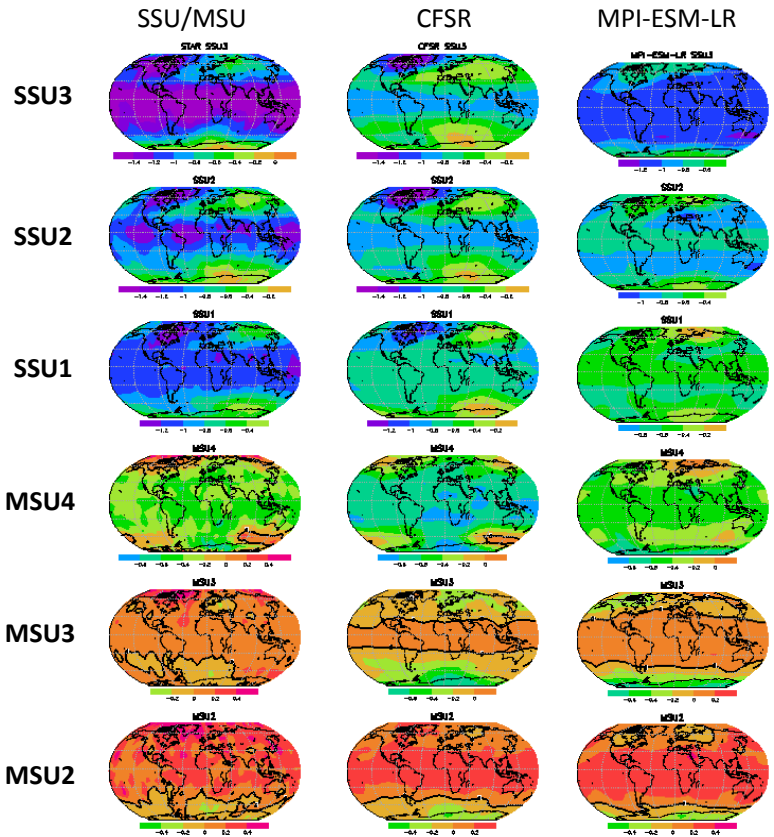

Fig. 5. Temperature trends (°C decade^{-1}) distribution in SSU/MSU observation (left panel), a reanalysis (middle panel) and a selected CMIP5 model (right panel).

ACPD
13, 3957–3992, 2013

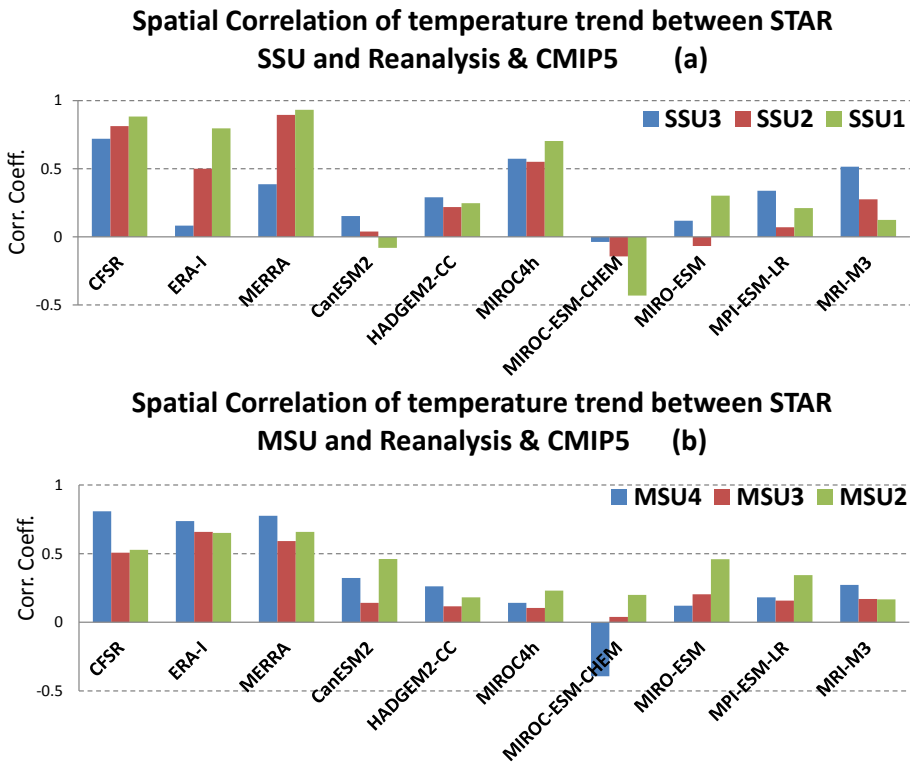

Fig. 6. Spatial correlation between SSU/MSU and CMIP5 model simulations/reanalyses, **(a)** SSU, **(b)** MSU. Note SSU1 ~ 3 and MSU2 ~ 4 represent the SSU/MSU observational layers.

ACPD
13, 3957–3992, 2013

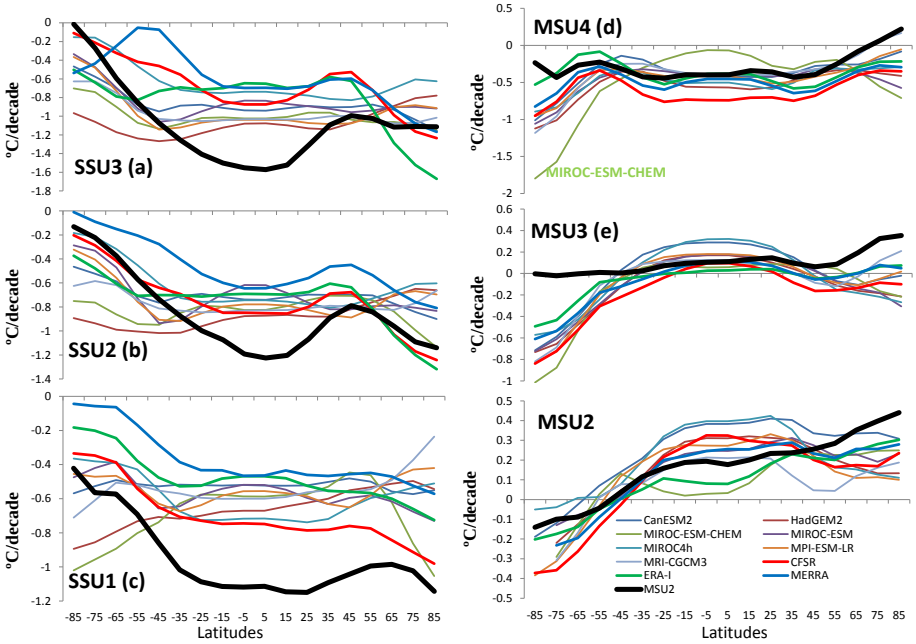

Fig. 7. Temperature trends (°C decade^{-1}) change with latitudes **(a)** SSU3, **(b)** SSU2, **(c)** SSU1, **(d)** MSU4 , **(e)** MSU3, **(f)** MSU2. Note SSU1 ~ SSU3 and MSU2 ~ MSU4 represent the layer of the SSU and MSU observations. Note SSU1 ~ 3 and MSU2 ~ 4 represent the SSU/MSU observational layers.

ACPD
13, 3957–3992, 2013

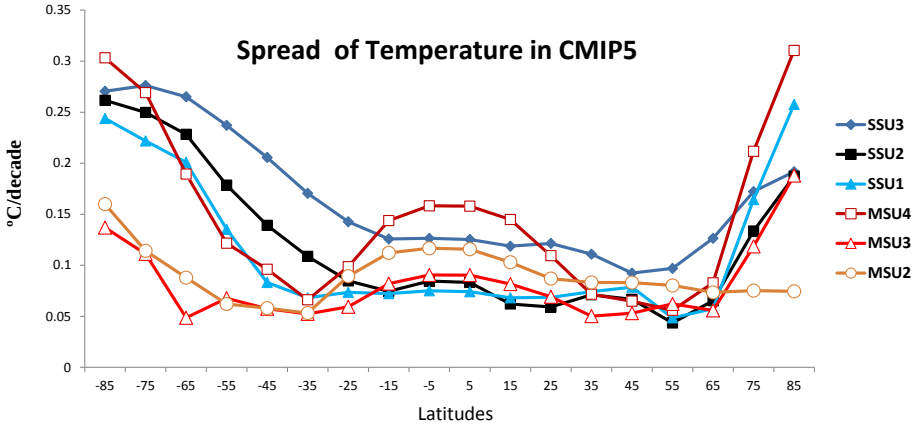

Fig. 8. Spread of temperature trends (°C decade^{-1}) change with latitudes in CMIP5 model simulations. Note SSU1 ~ SSU3 and MSU2 ~ MSU4 represent the layer of the SSU and MSU observations.

ACPD
13, 3957–3992, 2013

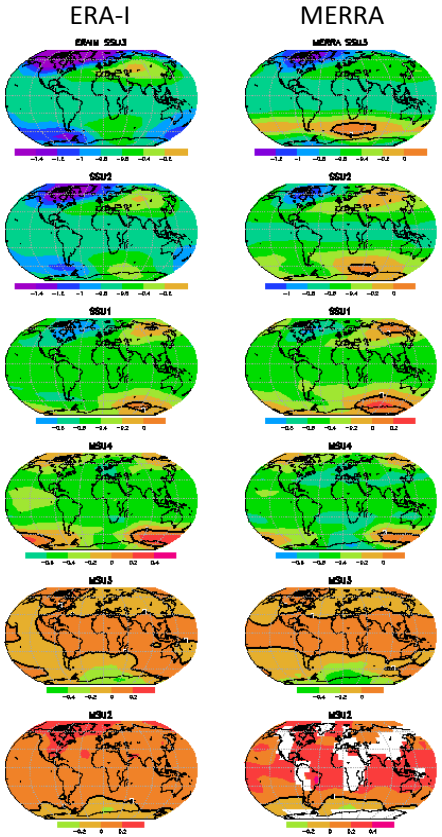

Fig. A1. Temperature trend (°C decade^{-1}) distribution in reanalysis. Left: ERA-I and right: MERRA.

ACPD
13, 3957–3992, 2013

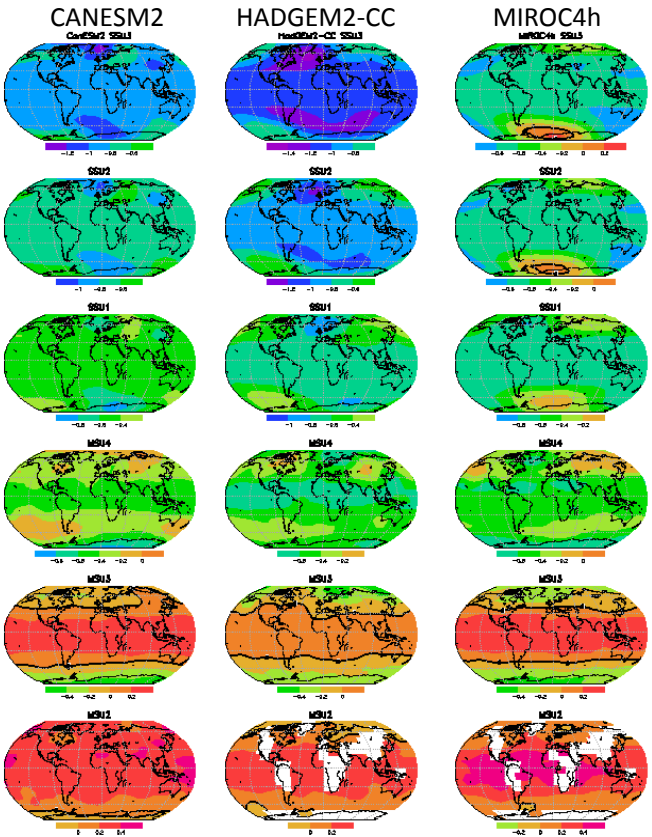

Fig. A2a. Temperature trend (°C decade^{-1}) distribution in the selected CMIP5 model. Left: CANESM2; middle: HADGEM2-CC; right: MIROC4h.

ACPD
13, 3957–3992, 2013

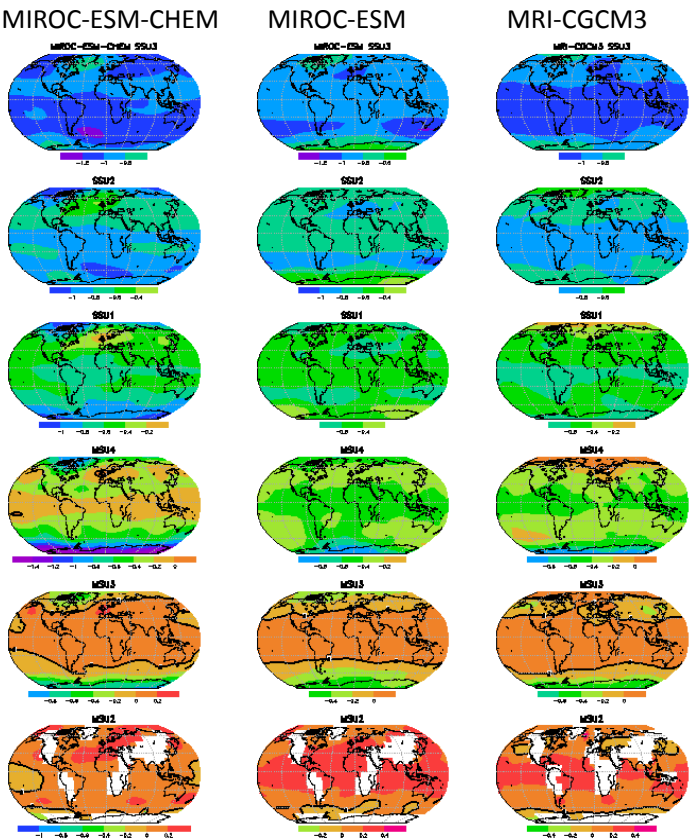

Fig. A2b. Temperature trend (°C decade^{-1}) distribution in the selected CMIP5 model. Left: MIROC-ESM-CHEM; middle: MIROC-ESM; right: MRI-CGCM3.

ACPD
13, 3957–3992, 2013